



A highly stable and efficient organic microcavity polariton laser

Julia Witt, Andreas Mischok, and Florian Le Roux, Humboldt Centre for Nano- and Biophotonics, Department of Chemistry, University of Cologne, Greinstr. 4-6, 50939 Cologne, Germany

Malte C. Gather¹, Humboldt Centre for Nano- and Biophotonics, Department of Chemistry, University of Cologne, Greinstr. 4-6, 50939 Cologne, Germany; Organic Semiconductor Centre, SUPA, School of Physics and Astronomy, University of St Andrews, North Haugh, St Andrews KY16 9SS, UK

Address all correspondence to Malte C. Gather at malte.gather@uni-koeln.de

(Received 9 October 2023; accepted 6 March 2024)

Abstract

With their remarkably low thresholds, organic polariton lasers are a promising alternative to organic photonic lasers. However, device stability remains a challenge, in part due to material degradation during deposition of the top dielectric mirror. We demonstrate polariton lasers based on 4,4'-Bis(4-(9H-carbazol-9-yl)styryl)biphenyl (BSBCz) as active material that achieve a low lasing threshold of $8.7 \mu\text{J}/\text{cm}^2$, and we show that a ZrO_2 protection layer between active layer and top mirror significantly improves stability. Optimized devices exhibit minimal degradation after 100,000 excitation pulses at 3.8 times above threshold. Our findings establish BSBCz as an attractive candidate for future injection driven polariton lasers.

Introduction

Polariton lasing occurs when polaritons, quasi-particles traditionally formed in planar microcavities through the hybridization of excitons and photons, scatter into a macroscopic ground state and subsequently decay coherently through one of the mirrors.^[1] Organic semiconductors represent an attractive family of materials for such devices as excited states in these materials take the form of Frenkel excitons which possess both large oscillator strengths and large binding energies, thus enabling room temperature operation.^[2,3] Organic polariton lasers now rival conventional, i.e. photonic, organic lasers in terms of performance, with their lasing thresholds now on par with their best photonic counterparts.^[4,5] Nonetheless, low photostability remains a major obstacle in the way of both practical application and the long-sought electrical injection. This stability critically hinges on the choice of the emissive material, the quality factor of the microcavity, and the fabrication process used. For optically pumped polariton lasing, the emissive material must possess specific attributes: a substantial oscillator strength, a short singlet decay rate, and a high photoluminescence quantum efficiency (PLQE).^[1] 4,4'-Bis(4-(9H-carbazol-9-yl)styryl)biphenyl (BSBCz) exhibits the above-mentioned properties and materials with structural similarity to BSBCz and solubilizing side-chains have been previously used to fabricate efficient polariton lasers.^[6,7] BSBCz is also particularly promising for the realization of an electrically pumped polariton laser since it displays a large stimulated emission cross-section, short triplet lifetime, and balanced charge transport.^[8,9] These advantageous features led to the groundbreaking work by Sandanayaka et al. who observed indications of current-injection lasing using an organic semiconductor and a distributed feedback (DFB) resonator.^[9,10]

While performance is key to the realization of electrical injection, device stability is usually the first obstacle in the way of any experiments aimed at electrical injection. In a low loss planar microcavity, the emissive layer is typically sandwiched between two distributed Bragg reflectors (DBRs) where the top DBR is fabricated using magnetron sputtering or electron beam evaporation, deposition techniques which can lead to severe degradation of both morphology and PLQE of the emissive layer. Various strategies have been brought forward to try and address this issue: the use of protective layers,^[11] thermal evaporation of the DBRs,^[4,12] or lamination rather than direct deposition of the top DBR.^[6,13] However, these techniques often strike an undesirable balance between laser performance and stability when both actually need to be maximized.

In this work, we fabricate high Q-factor microcavities containing a BSBCz layer doped at 50wt% into a host matrix of CBP using two DBRs fabricated using magnetron sputtering. The energy of the lower polariton (LP) is tuned to the (0–1) vibronic peak, a desirable feature for highly efficient polariton lasing.^[6,14] We explore protecting the organic layer from direct sputtering by adding different protecting layers which we deposit by either thermal evaporation or atomic layer deposition (ALD). Using ALD- ZrO_2 as protection layer and as the first high-index layer of the top DBR, we achieve polariton lasing at a low threshold of $9.0 \mu\text{J}/\text{cm}^2$ together with a dramatically increased stability, observing only minimal degradation after 100,000 excitation pulses at an excitation energy 3.8 times above the lasing threshold, compared to a drop in the intensity of the polariton laser emission to below 70% of the initial intensity after only 22,500 excitation pulses without this protection. This work shows that the realization of a low-threshold and highly stable organic polariton laser is indeed possible and

thus represents a further step in the direction of an electrically driven organic polariton laser.

Results

We first tested a conventional polariton laser structure, in which the active organic layer was sandwiched between two Bragg-mirrors and no protection layer was used (device **D1**, [Fig. 1(a)]). A blend of BSBCz with 4,4'-Bis(carbazol-9-yl) biphenyl (CBP) (50wt%) was used as the active layer, as this is known to show good compatibility and stability while retaining the favorable horizontal molecular orientation of BSBCz.^[4,15] The high doping concentration was chosen to guarantee a high coupling strength and high polariton density in the device, which is required for polariton lasing. The emissive layer was sandwiched between two DBRs, each consisting of 21 alternating lambda-quarter layers of Ta₂O₅/SiO₂ at a design wavelength of 465 nm, offering >99% reflectivity.^[16] Figure 1(b) shows transfer matrix simulations and experimental measurements of the angle resolved reflectivity of the structure, as well as the calculated position of the cavity mode and the fitted position of the lower polariton branch (LPB). It shows the deviation of the simulated and experimental data from the behavior of a bare cavity and instead how the spectra follow the shape of the flat LP mode (also see Supplementary Information S1). Given the coupling strength (and thus Rabi-splitting) we observe here and the limited width of the DBR stop-band, the upper polariton is not clearly visible. Such a behavior has also been described in earlier reports on polariton lasers using a similar material.^[6] Cao et al. describe such systems through coupling of the (upper) polariton branch with the photonic sidebands of the DBR, forming Bragg-polaritons. We also find this behavior in the simulated and measured reflectivity maps in [Fig. 1(b)]. However, due to this additional coupling, it is not possible to determine the position and shape of the upper polariton branch (UPB).

Non-resonant pumping of the exciton reservoir was performed at a wavelength of 355 nm (see absorption and photoluminescence spectrum in Supplementary Information, Fig. S2). Once the pump pulse energy was increased beyond the lasing threshold, a characteristic collapse of the size of the emission spot was observed [Fig. 1(c and d)]; Supplementary Information, Discussion S1).

Next, momentum space micro-photoluminescence spectroscopy was performed while increasing the excitation pulse energy in steps going from 13.6 pJ (4.3 μJ/cm²) up to 34.8 pJ (11.1 μJ/cm²). A gradual change of the emission from the LPB to a blue-shifted and flat lasing emission was observed [Fig. 2(a–d)], in line with the expected behavior for polariton lasing.^[1,13,17,18] Specifically, the spectrum recorded at an excitation energy of 13.6 pJ and 17.0 pJ [Fig. 2(a and b)] followed the LPB dispersion closely. At 27.7 pJ [Fig. 2(c)], the emission spectrally narrowed and flattened, slightly blue-shifting from the ground state of the LPB, a trend then increased at 34.8 pJ [Fig. 2(d)], also see Supplementary Information, Fig. S3). The lasing characteristics are further summarized in [Fig. 2(e–f)]. The lasing threshold was obtained using a double logarithmic input–output curve, which shows a steep, nonlinear-increase in emission intensity at $E_{th} = 27.3$ pJ (8.7 μJ/cm², [Fig. 2(g)]).

This result is in line with previous reports on lasing in devices containing a solution processable organic material that bears structural similarities to BSBCz.^[6] Nevertheless, such organic polariton lasers previously showed poor long-term stability at pump energies located significantly above threshold.^[6,11,19,20] One explanation is that the fabrication of the top DBR damages the emissive layer. For example, during sputtering, molecules are ejected from a target with high kinetic energy and can damage the organic layer and thus decrease the quantum efficiency or stability of the previously deposited materials.^[6] In addition, during DBR deposition, a substantial amount of UV radiation is created, leading to potential photobleaching. Besides, sputtered oxide layers only provide a small degree of protection against oxygen and water vapour

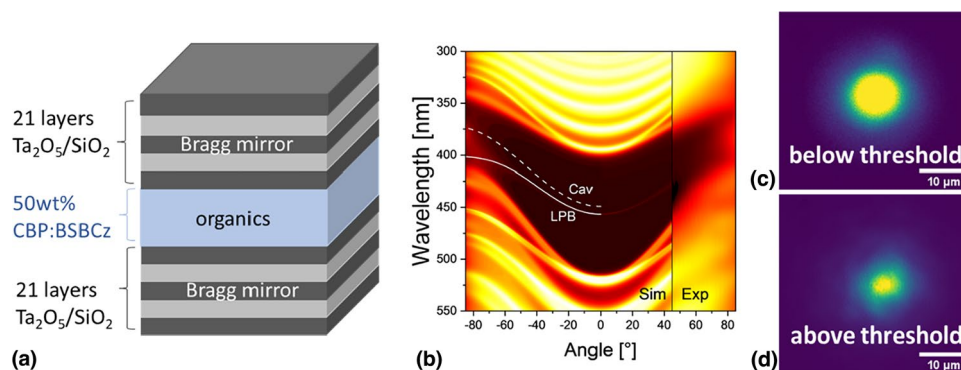


Figure 1. (a) Schematic illustration of device **D1**. An organic layer of 50 wt% CBP:BSBCz is sandwiched between two Bragg-mirrors containing 21 alternating layers of Ta₂O₅/SiO₂. (b) Transfer matrix simulation and experimental data of the angle resolved reflectivity of a DBR cavity containing BSBCz. The lower polariton branch is clearly visible and shown together with the cavity mode. Representative micro-graph of the real-space emission (c) below and (d) above the lasing threshold.

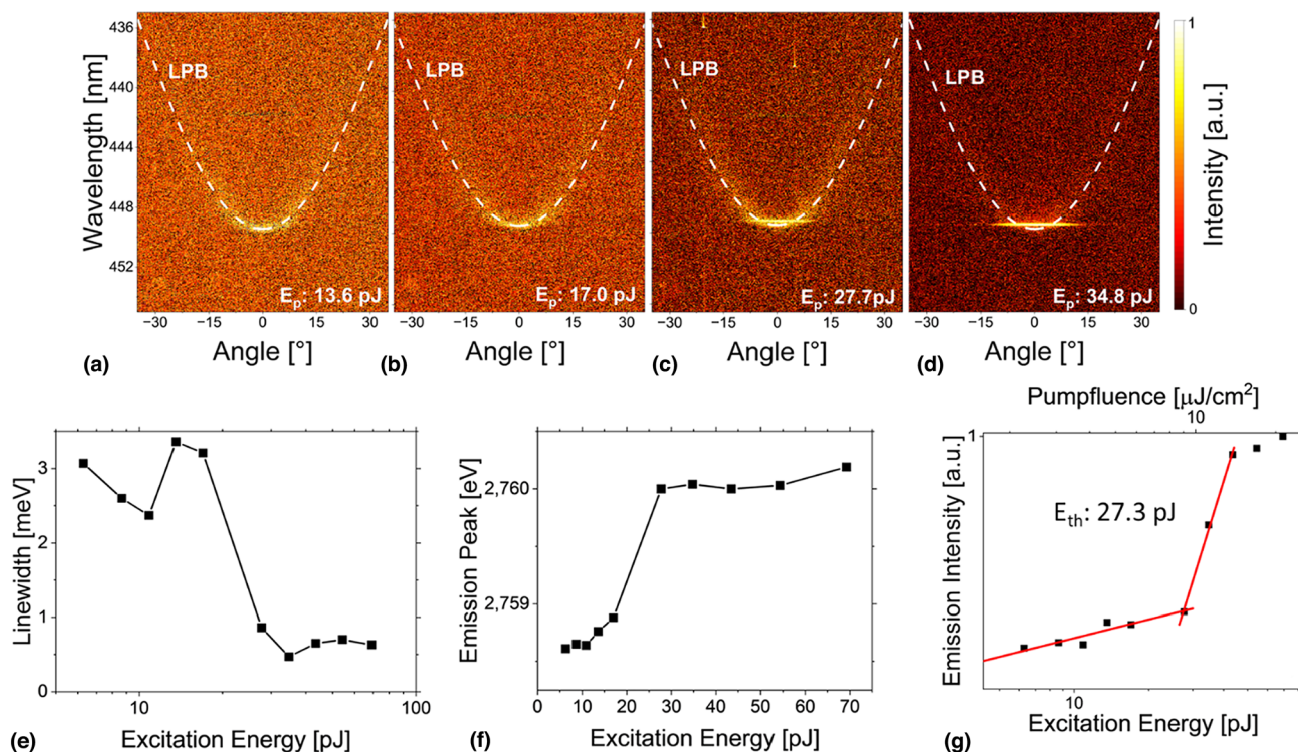


Figure 2. Angle-resolved photoluminescence measurements for increasing excitation energies; (a) 13.6 pJ, (b) 17.0 pJ, (c) 27.7 pJ and (d) 34.8 pJ. A coupled oscillator calculation of the position and dispersion of the fitted LPB (dashed white line) was fitted to the measured data. (e) Emission-linewidth, (f) blue-shift of the emission peaks and (g) input-output characteristics of the laser, all of which show a clear threshold behavior.

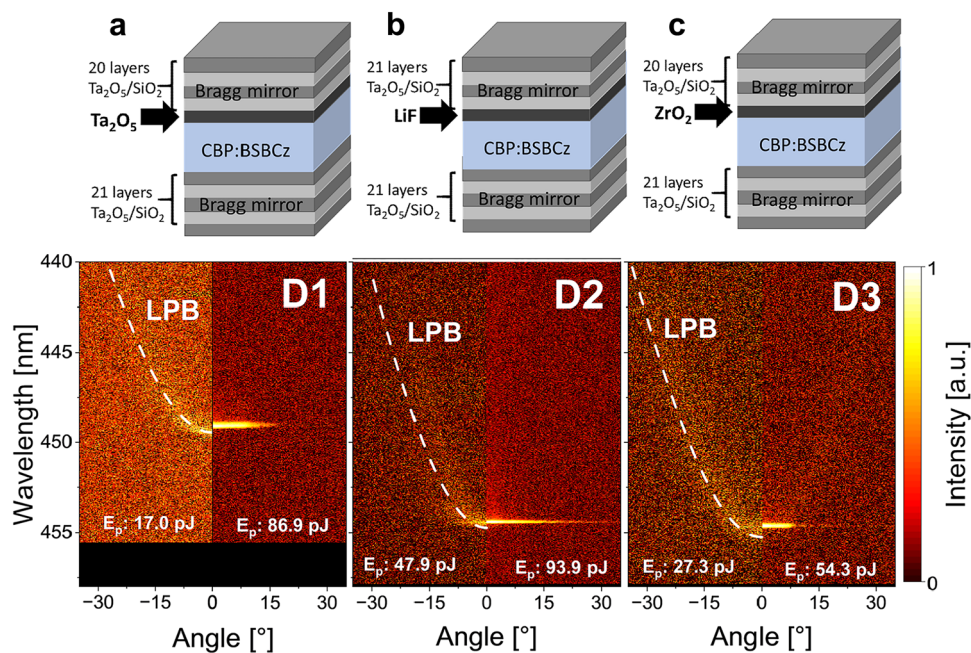


Figure 3. Top: Schematic structure of the polariton lasers with different protection layers studied in this work: (a) device **D1** no protection layer, (b) device **D2** with additional LiF layer fabricated using vacuum evaporation, and (c) device **D3** with ALD-deposited ZrO_2 layer, which replaces the first Ta_2O_5 layer of the Bragg mirror. Bottom: Angle-resolved photoluminescence measurements of the corresponding devices below (left) and above (right) the lasing threshold. The position and dispersion of the LPB as predicted by a coupled oscillator model simulation is overlaid onto the sub-threshold data (white dashed line) in each case.

for the active layer. To protect the organic layer from such damage, we implemented a protection layer of either thermally evaporated LiF (device **D2**) or ZrO₂ deposited by ALD (device **D3**) between the active layer and the top DBR (Fig. 3, for specific layer thicknesses and further discussion, see Supporting Information, Table 1 and Discussion S2). LiF is known as efficient encapsulation layer for various other devices^[21] and has been successfully used to enhance the stability of polyfluorene-based polariton lasers.^[11] It can be thermally evaporated directly on the organic layer leading to better thermal insulation and protecting the active layer during further processing. LiF however exhibits a relatively small refractive index and thus is not ideal as first DBR layer. Conversely, ZrO₂ can be processed using atomic layer deposition (ALD) at moderate temperatures (80°C), shows a refractive index comparable to Ta₂O₅, and is thus ideally suited to replace the first DBR layer without compromising the optical quality of the device. The use of ALD leads to very high quality, conformal, uniform films of well-controlled material composition. Therefore, ALD of different materials is routinely used for thin film encapsulation of organic optoelectronic devices.^[22–24] In comparison, oxide films grown through magnetron sputtering or electron beam evaporation are often more porous, less dense, directional, and show slightly reduced refractive index, depending on the processing conditions used. Thus, the first layer (Ta₂O₅) of the top DBR was replaced by an ALD deposited layer of ZrO₂. After the addition of either protection layer, the top DBR was sputtered on top. The devices were not encapsulated further, and while device fabrication was carried out under vacuum and inert gas glovebox, all measurements were performed in air under ambient conditions.

All spectra show polariton lasing characteristics such as narrowing and blue-shift of the emission above a certain excitation threshold (also see Supplementary Information, Fig. S4 and Discussion S3). While the emission from the reference device **D1** peaks at a wavelength of 450 nm, the protected devices show emission at 454 nm (LiF, **D2**) and 455 nm (ZrO₂, **D3**). These minor deviations are due to the use

of different fabrication methods, as well as potential interactions with the added materials. The devices also differ in their lasing thresholds (see Supplementary Information, Fig. S5). The unprotected device **D1** and the device containing ZrO₂ **D3** exhibit similar thresholds at 27.3 pJ (8.7 μJ/cm²) and 28.7 pJ (9.0 μJ/cm²), demonstrating that replacing the first Ta₂O₅ layer by ZrO₂ has no significant influence on the lasing threshold. The use of LiF as protection layer increases the lasing threshold to 56.8 pJ (17.8 μJ/cm²), which is likely related to a lower optical quality of the top DBR, caused by the addition of a third low-index material into the optical cavity. These values are among the lowest thresholds reported for organic polariton lasing thus far.^[11,25]

The other crucial characteristic of these lasers is their stability. Each laser was exposed to a series of excitation pulses at a repetition rate of 250 Hz and a pulse energy of 108.6 pJ, which is above the lasing threshold of all devices, and their degradation was monitored by analyzing the decay of the intensity of the main lasing peak (Fig. 4).

The results show that the implementation of protecting layers leads to a drastic change in operational lifetime. The emission of device **D1** (where a pump pulse energy of 108.6 pJ corresponds to 4 times the lasing threshold) decreased to 70% of its initial intensity (LT₇₀) within 1.5 min, corresponding to 22,500 excitation pulses. The intensity decreased approximately linearly with time. The additional short-term fluctuations in intensity are likely linked to peak-to-peak variations in the pulse energy from the pump laser and or to noise in the measurement.

In comparison, device **D2** showed a significantly shorter operation lifetime. Even at a lower repetition rate of 50 Hz, the device had an LT₇₀ of only 0.5 min or 1,500 excitation pulses. This is a surprisingly short lifetime since LiF is commonly used in encapsulation as well as for DBR fabrication.^[6,11] The ALD-encapsulated device **D3** proved to be the most stable device, with an LT₇₀ of 9.5 min at 250 Hz or 142,500 excitation pulses. (The pump pulse energy of 108.6 pJ corresponded to 3.8 times the lasing threshold

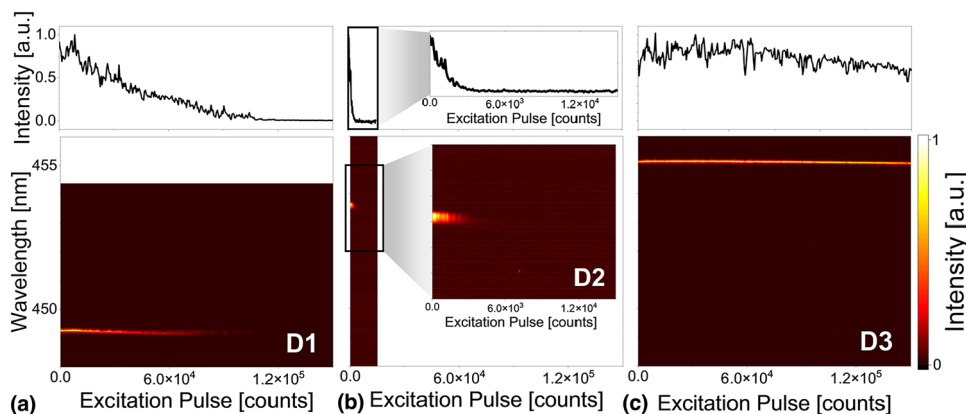


Figure 4. Measurements of operational lifetime of the three different devices above their lasing thresholds for (a) the device with unprotected organic layer (**D1**), (b) the device with LiF-protected organic layer (**D2**) and (c) the device with ZrO₂-protected organic layer (**D3**).

for device **D3**.) This represents one of the highest reported lifetimes of polariton lasers, even when compared to recent reports.^[20] In addition, neither significant spectral diffusion nor photobleaching were observed (see Supplementary Information Fig. S6). We therefore conclude that the high quality of the ALD-grown ZrO₂ layer not only protects the active organic layer from damage during deposition of the top DBR but that it also acts as an efficient barrier for oxygen, further reducing degradation and photobleaching. This simple encapsulation layer thus shows a significant improvement in operational lifetime at no cost to cavity quality nor lasing threshold and can be used for any kind of organic emitter that is stable under ALD processing conditions i.e. that can sustain a temperature of up to 80°C.

Conclusion

In summary, an improvement of more than 90% in operational lifetime (up to an LT₇₀ of 142,500 excitation pulses) was achieved by replacing the first sputtered Ta₂O₅ layer of the top dielectric mirror by an ALD-deposited ZrO₂ layer. Sputtering Ta₂O₅ directly onto the organic layer was found to be more damaging than depositing ZrO₂ via ALD. The drastic improvement in stability was realized at no significant cost in terms of laser performances as a low lasing threshold of 28.7 pJ (9.0 μJ/cm²) was also seen for the ZrO₂ protected device, almost equal to the threshold measured for the device with no protection layer, 27.3 pJ (8.7 pJ/cm²). These values are compatible with thresholds found in the literature for similar devices.^[6] We have therefore demonstrated that replacing the first sputtered layer of the top dielectric mirror with a protection layer deposited via ALD is a beneficial strategy for the development of low-threshold, highly stable organic polariton lasers.

Methods Fabrication

Layers of LiF, CBP and BSBCz were produced by vacuum sublimation at a rate of 0.3 Å/s and a base pressure of 10⁻⁷ mbar (*EvoVac, Angstrom Engineering*). The evaporation rates and layer thicknesses were monitored via a quartz crystal microbalance. The Bragg-mirrors were fabricated on glass substrates via radiofrequency magnetron sputtering (also *EvoVac, Angstrom Engineering*, but configured for sputtering) of 21 alternating Ta₂O₅ and SiO₂ layers (51.2 and 75 nm, respectively) at a base pressure of ≈10⁻⁷ mbar and a process pressure 2.7 × 10⁻³ mbar and an Argon flow of 18 sccm (SiO₂) or a process pressure of 5.3 × 10⁻³ mbar and a flow of 18 sccm Argon, 4 sccm Oxygen (Ta₂O₅). The 64 nm thick ZrO₂ layer was produced via ALD (*Savannah, Veeco*). For this, Tetrakis(dimethylamino)zirconium (TDMAZr) was used as precursor and pulsed for 0.07 s and H₂O pulsed 0.015 s in 383 cycles at 80°C reactor temperature.

Characterization

PL spectra were measured using Fourier imaging spectroscopy by imaging the back focal plane of a 40× objective (numerical aperture 0.75, Nikon Plan Fluor), set up on a commercial inverted microscope stand in reflection configuration (Nikon Eclipse Ti2-E). The third harmonic generation (THG) output of a diode-pumped Nd:YAG laser system (*PL2210A, Ekspla*), with wavelength 355 nm, repetition rate 50 or 250 Hz, and pulse duration 25 ps was used for excitation. Linear polarization of the pump was set by placing a Glan-Taylor polarizer (*GT10-A, Thorlabs*) before the objective. The emitted light was directed towards the entrance of a spectrograph (*Shamrock SR-500i-D2-SiL, Andor*) equipped with an 1800 lines mm⁻¹ grating blazed at 500 nm and the PL spectra were imaged on an EM CCD camera (*Newton 971, Andor*) providing a spectral resolution of 40 pm (~300 μeV at 2.67 eV).

Author contributions

JW and AM fabricated devices. JW and FLR recorded laser characteristics. AM and MCG initiated the study. All authors discussed the results and contributed to writing of the manuscript.

Funding

The authors acknowledge support by the Deutsche Forschungsgemeinschaft (Research Training Group “TIDE”, RTG2591). M.C.G. and F.L.R. acknowledge funding from the Alexander von Humboldt Foundation (Humboldt Professorship to M.C.G. and Humboldt Fellowship to F.L.R.). A.M. acknowledges funding from the European Union’s Horizon 2020 research and innovation programme under Marie Skłodowska-Curie grant agreement No. 101023743 (PolDev). M.C.G. acknowledges funding from the European Research Council under the European Union’s Horizon Europe Framework Programme/ERC Advanced Grant agreement No. 101097878 (HyAngle).

Data availability

The data that support the findings of this study are openly available in University of St Andrews Repository at <https://doi.org/10.17630/8acd831e-ad09-414d-ab1e-f0b496595105>.

Declarations

Conflict of interest

On behalf of all authors, the corresponding author states that there is no conflict of interest.

Supplementary Information

The online version contains supplementary material available at <https://doi.org/10.1557/s43579-024-00543-6>.

Open Access

This article is licensed under a Creative Commons Attribution 4.0 International License, which permits use, sharing, adaptation, distribution and reproduction in any medium or format, as long as you give appropriate credit to the original author(s) and the source, provide a link to the Creative Commons licence, and indicate if changes were made. The images or other third party material in this article are included in the article's Creative Commons licence, unless indicated otherwise in a credit line to the material. If material is not included in the article's Creative Commons licence and your intended use is not permitted by statutory regulation or exceeds the permitted use, you will need to obtain permission directly from the copyright holder. To view a copy of this licence, visit <http://creativecommons.org/licenses/by/4.0/>.

References

1. J. Keeling, S. Kéna-Cohen, Bose-einstein condensation of exciton-polaritons in organic microcavities. *Annu. Rev. Phys. Chem.* **71**, 435–459 (2020)
2. S.F. Alvarado, P.F. Seidler, D.G. Lidzey, D.D.C. Bradley, Direct determination of the exciton binding energy of conjugated polymers using a scanning tunneling microscope. *Phys. Rev. Lett.* **81**, 1082–1085 (1998)
3. R.N. Marks, J.J.M. Halls, D.D.C. Bradley, R.H. Friend, A.B. Holmes, The photo-voltaic response in poly(p-phenylene vinylene) thin-film devices. *J. Phys. Condens. Matter* **6**, 1379–1394 (1994)
4. Y. Hu et al., High performance planar microcavity organic semiconductor lasers based on thermally evaporated top distributed Bragg reflector. *Appl. Phys. Lett.* (2020). <https://doi.org/10.1063/5.0016052>
5. A. Mischok et al., Photonic confinement in laterally structured metal-organic microcavities. *Appl. Phys. Lett.* (2014). <https://doi.org/10.1063/1.4892533>
6. T. Ishii et al., Low-threshold exciton-polariton condensation via fast polariton relaxation in organic microcavities. *Adv. Opt. Mater.* **10**, 2102034 (2022)
7. M. Wei et al., Low threshold room temperature polariton lasing from fluorene-based oligomers. *Laser Photonics Rev.* **15**, 1–8 (2021)
8. Q. Ou, Q. Peng, Z. Shuai, Computational screen-out strategy for electrically pumped organic laser materials. *Nat. Commun.* **11**, 1–10 (2020)
9. A.S.D. Sandanayaka et al., Quasi-continuous-wave organic thin-film distributed feedback laser. *Adv. Opt. Mater.* **4**, 834–839 (2016)
10. A.S.D. Sandanayaka et al., Indication of current-injection lasing from an organic semiconductor. *Appl. Phys. Express* (2019). <https://doi.org/10.7567/1882-0786/ab1b90>
11. S.K. Rajendran et al., Low threshold polariton lasing from a solution-processed organic semiconductor in a planar microcavity. *Adv. Opt. Mater.* **7**, 1–7 (2019)
12. M. Anni et al., Organic microcavities based on thermally evaporated TeO_x-LiF dielectric mirrors. *Phys. E Low-Dimens. Syst. Nanostruct.* **13**, 451–454 (2002)
13. C.P. Dietrich et al., An exciton-polariton laser based on biologically produced fluorescent protein. *Sci. Adv.* **2**, 1–8 (2016)
14. F. Le Roux, A. Mischok, D.D.C. Bradley, M.C. Gather, Efficient anisotropic polariton lasing using molecular conformation and orientation in organic microcavities. *Adv. Funct. Mater.* **32**, 2209241 (2022)
15. D. Yokoyama, A. Sakaguchi, M. Suzuki, C. Adachi, Horizontal orientation of linear-shaped organic molecules having bulky substituents in neat and doped vacuum-deposited amorphous films. *Org. Electron.* **10**, 127–137 (2009)
16. H.T. Assafli, A.H. Abdulhadi, W.Y. Nassir, Design high efficient reflectivity of distributed bragg reflectors. *Iraqi J. Laser, Part A* **15**, 13–18 (2016)
17. T. Yagafarov et al., Mechanisms of blueshifts in organic polariton condensates. *Commun. Phys.* **3**, 1–10 (2020)
18. S. Kéna-Cohen, S.R. Forrest, Room-temperature polariton lasing in an organic single-crystal microcavity. *Nat. Photonics* **4**, 371–375 (2010)
19. A.S.D. Sandanayaka et al., Toward continuous-wave operation of organic semiconductor lasers. *Sci. Adv.* **3**, 1–9 (2017)
20. K.E. McGhee, R. Jayaprakash, K. Georgiou, S.L. Burg, D.G. Lidzey, Polariton condensation in a microcavity using a highly-stable molecular dye. *J. Mater. Chem. C* **10**, 4187–4195 (2022)
21. Y. Peng et al., Thin-film encapsulation of organic electronic devices based on vacuum evaporated lithium fluoride as protective buffer layer. *Appl. Phys. A Mater. Sci. Process.* **123**, 1–7 (2017)
22. S. Sarkar, J.H. Culp, J.T. Whyland, M. Garvan, V. Misra, Encapsulation of organic solar cells with ultrathin barrier layers deposited by ozone-based atomic layer deposition. *Org. Electron.* **11**, 1896–1900 (2010)
23. F. Nehm et al., Atomic layer deposited TiO_x/AlO_x nanolaminates as moisture barriers for organic devices. *Org. Electron.* **38**, 84–88 (2016)
24. S.W. Seo, E. Jung, H. Chae, S.M. Cho, Optimization of Al₂O₃/ZrO₂ nanolaminate structure for thin-film encapsulation of OLEDs. *Org. Electron.* **13**, 2436–2441 (2012)
25. M. Wei et al., Low threshold room temperature polariton lasing from fluorene-based oligomers. *Laser Photonics Rev.* **15**, 2100028 (2021)

Publisher's Note Springer Nature remains neutral with regard to jurisdictional claims in published maps and institutional affiliations.